AIP Journal of Applied Physics

Many-body design of highly strained GaInNAs electroabsorption modulators on GaInAs ternary substrates

Takeshi Fujisawa, Masakazu Arai, and Fumiyoshi Kano

Citation: Journal of Applied Physics **107**, 093107 (2010); doi: 10.1063/1.3360937
View online: http://dx.doi.org/10.1063/1.3360937
View Table of Contents: http://scitation.aip.org/content/aip/journal/jap/107/9?ver=pdfcov
Published by the AIP Publishing

Many-body design of highly strained GaInNAs electroabsorption modulators on GaInAs ternary substrates

Takeshi Fujisawa,[a] Masakazu Arai, and Fumiyoshi Kano
NTT Photonics Laboratories, NTT Corporation, 3-1 Morinosato-Wakamiya, Atsugi, Kanagawa 243-0198, Japan

(Received 15 December 2009; accepted 10 February 2010; published online 4 May 2010)

Electroabsorption in highly strained GaInAs and GaInNAs quantum wells (QWs) grown on GaInAs or quasi-GaInAs substrates is investigated by using microscopic many-body theory. The effects of various parameters, such as strain, barrier height, substrate composition, and temperature are thoroughly examined. It is shown that the value of the absorption coefficient strongly depends on the depth of the QWs under large bias electric field due to the small overlap integral of wave functions between the conduction and valence bands. The use of GaInNAs QWs makes the strain in the well layer very small. Further, the effective quantum-well depth is increased in GaInNAs QWs due to the anticrossing interaction between the conduction and N-resonant bands, making it possible to obtain larger absorption coefficient under large bias electric fields without using wide-band gap materials for barriers. © *2010 American Institute of Physics*. [doi:10.1063/1.3360937]

I. INTRODUCTION

Uncooled and high-speed lightsources around 1.5 and 1.3 μm bands have attracted considerable attention recently. Several international standards employing these lightsources (such as, 10 Gbit/s and 40 Gbit/s for 1.5 μm band, and 25 Gbit/s and 40 Gbit/s for 1.3 μm band) are being discussed for the next-generation network.[1] They require uncooled, thermo-electric-cooler-free modulator integrated lightsources for low-cost optical transponders. To realize such a lightsource, AlGaInAs/InP-based directly modulated distributed feedback (DFB) lasers and electroabsorption modulators (EAMs) integrated with DFB (EADFB) lasers have been demonstrated.[2–5] These AlGaInAs-based devices have better temperature characteristics than their conventional GaInAsP-based counterparts, but Al-based material has the problem of oxidization, which affects the performance and reliability.

It has been shown that GaAs substrate-based semiconductor quantum well (QW) lasers have excellent temperature characteristics compared with those of InP-substrate-based QW lasers due to their large conduction band offset, ΔE_c. The drawback of these lasers is that a huge amount of strain is required in the well layer to obtain 1.3 μm light. One way to overcome this problem is to use GaInAs or quasi-GaInAs substrate.[6–12] The larger the In content of the substrate (x_{sub}) is, the smaller the strain of the well layer becomes. So far, we have fabricated highly strained QW lasers on GaInAs or quasi-GaInAs substrate and obtained around 1.3 μm lasing.[12–17] By using ternary substrates, the strain required for 1.3 μm lasing can be significantly reduced and we have demonstrated uncooled (up to 100 °C), 10 Gbit/s direct modulation.[15–17] Another approach is to use GaInNAs QWs.[18–21] By incorporating a small amount of N (usually $<2\%$) into the GaInAs well layer, the band gap of the material is dramatically reduced. Many theoretical and experimental studies have shown the usefulness of GaInNAs laser diodes on GaAs substrates for high-temperature operation compared with conventional lasers grown on InP substrate.

The EADFB laser is another promising candidate for compact and low-cost modulator integrated lightsources. In an EAM, the redshift of the absorption edge of the QWs under a bias voltage (quantum confined Stark effect) is utilized for modulation. For EADFB lasers since the modulator can be optimized separately, extinction ratio enhancement and chirp management are easier than for directly modulated lasers. Since these characteristics strongly depend on the layer structure of the QWs, the theoretical study of the optical properties of QWs is indispensable for optimization. However, a detailed theoretical investigation of electroabsorption in QWs grown on GaInAs ternary substrates has not been done.

In this paper, electroabsorption in highly strained QWs grown on GaInAs or quasi-GaInAs substrates is investigated. The effects of various parameters, such as strain, barrier height, substrate composition, and temperature are thoroughly examined. Microscopic many-body theory[22–26] was used to calculate the absorption spectra of QWs. The theory enables us to exclude unknown fitting parameters from the simulation and gives not only qualitative, but also quantitative results, which are comparable to experiment.[24–26] It is shown that the value of absorption coefficient strongly depends on the depth of the QWs under large bias electric field, showing that careful design of QWs is necessary to ensure sufficient absorption. The use of GaInNAs QWs makes the strain in the well layer very small. Further, the effective QW depth is increased in GaInNAs QWs due to the anticrossing interaction between the conduction and N-resonant bands, making it possible to obtain large absorption coefficient under large bias electric fields without using wide-band gap materials for barriers.

II. THEORY

We consider QWs grown on a (001) GaAs or GaInAs substrates where the growth direction is z. The well layer is

[a]Electronic mail: fujisawa@aecl.ntt.co.jp.

GaInAs or GaInNAs, the barrier layer is GaInAs or AlGaInAs, and the cladding layer is GaInP. The barrier and cladding layers are lattice-matched. The strain and the thickness of the well layer are ε_w and L_w, respectively. Only compressive strain is considered in this paper. All the material constants and the interpolation scheme for compound materials other than GaInNAs used in this paper are extracted from Ref. 27. For GaInNAs QWs, band parameters are determined as in Refs. 20 and 25. Band structures of QWs are calculated by 10-band $\boldsymbol{k \cdot p}$ theory (band anticrossing model) specially formulated for highly strained materials.[25] In this model, the conduction band is coupled to a N-resonant band. The conduction sub-band energy becomes small due to the anticrossing with the N-resonant band. In this case, there is a possibility that the sub-band energy is lower than the bottom energy of the conduction band [later shown in Fig. 9(a)]. We assume that the bias electric field is effective only in the well region and the band offset is constant under the electric field. This assumption is valid if the barrier height is large.

For the absorption spectra of QWs, although conventional free-carrier theory (FCT) based on Fermi's golden rule gives a simple explicit formula, it is well-known that the magnitude and position of absorption spectra highly depend on the broadening function (Gaussian, Lorentzian, etc) and the value of relaxation time. For EAM design, in addition to the magnitude, the position of absorption spectra is also very important since the detuning from the lasing wavelength largely affects the total device performance.[2–4] Therefore, we used microscopic many-body theory for the calculation of absorption spectra. By formulating the problem on the basis of second quantization, the so-called following semiconductor Bloch equation[22] can be derived

$$\frac{dp_{k_t}}{dt} = -i\omega_{k_t} p_{k_t} - i\Omega_{k_t}(f_{ek_t} + f_{hk_t} - 1) + \left.\frac{\partial p_{k_t}}{\partial t}\right|_{\text{col}}, \qquad (1)$$

where p_{kt} is the microscopic polarization, $\hbar\omega_{kt}$ is the renormalized transition energy, and f_{ekt} and f_{hkt} are the Fermi–Dirac distributions for electrons and holes. The final term in Eq. (1) is the scattering contribution. (For the details of each term, see Ref. 23.) By solving Eq. (1), the microscopic polarization is calculated and a macroscopic polarization, P, is obtained by summing the microscopic polarization over all the states. The macroscopic polarization is related to material absorption through Maxwell's equations as

$$g(\hbar\omega) = \mathrm{Im}\left(\frac{P}{\varepsilon_0 n_B^2 E_0}\right) = \mathrm{Im}\left(\frac{2}{\varepsilon_0 n_B^2 E_0 V}\sum_{k_t} \mu_{k_t}^* p_{k_t}\right), \qquad (2)$$

where ε_0 is the permittivity in vacuum, n_B is the background refractive index, V is the volume, μ_{kt} is the dipole matrix element, and E_0 is the electric field of light. The theory enables us to account for various important physical phenomena for EAM design, such as the absorption peak due to excitons, band gap renormalization, and the collapse of the absorption peak due to Coulomb screening effects, which cannot be considered in FCT.

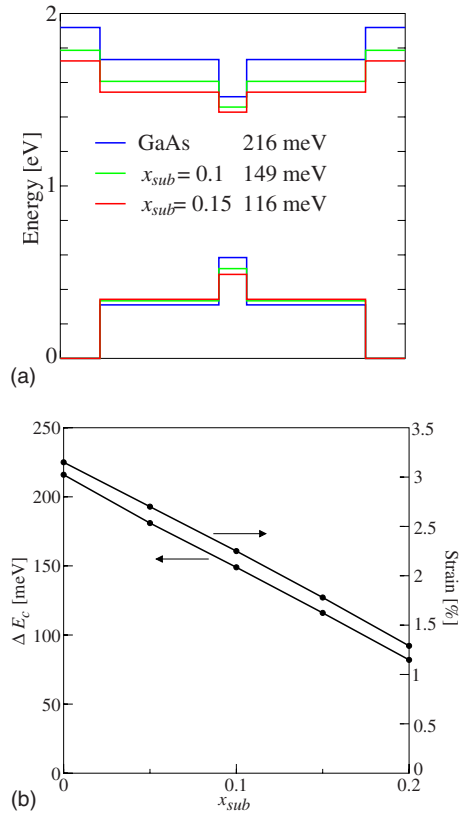

FIG. 1. (Color online) (a) Potential distributions of GaInAs/GaInAs QWs. (b) Strain required in the well layer and ΔE_c as a function of x_{sub}.

III. ELECTROABSORPTION IN HIGHLY STRAINED GAIN(N)AS/(AL)GAINAS QWS

A. Effects of substrate composition

Throughout the paper, the well thickness is fixed to $L_w = 7$ nm. The value of strain was chosen for the band gap wavelength between the first conduction and valence subbands (C1V1 wavelength) of 1.24 μm at 25 °C, and only TE mode absorption is considered.

Here, we consider GaInAs/GaInAs QWs. Figure 1(a) shows the potential distributions of QWs for the substrates with $x_{\text{sub}}=0$ (GaAs), 0.1, and 0.15. The QW depth becomes large for substrate with smaller x_{sub}. Figure 1(b) shows the strain required for a well and ΔE_c as a function of x_{sub}. Although ΔE_c is large for GaAs substrates, the strain exceeds 3%, which is very difficult for the crystal growth. Figure 2(a) shows the absorption spectra at 25, 55, and 85 °C for GaAs substrate without bias electric fields. For each temperature, the absorption spectra are plotted for three carrier densities. The magnitude of absorption coefficient is similar for different temperatures since both the well and barrier layers are redshifted simultaneously and the QW depth does not changed very much. For different carrier densities, the absorption spectra are drastically changed because of the collapse of the absorption peaks due to excitons. This phenomenon is important for the design of EAM since under high bias electric fields, the carrier density in a QW increases because the EAM absorbs light and generates electron-hole pairs. Figure 2(b) shows the absorption spectra of GaInAs/GaInAs QWs for the substrate with $x_{\text{sub}}=0.1$. The absorption

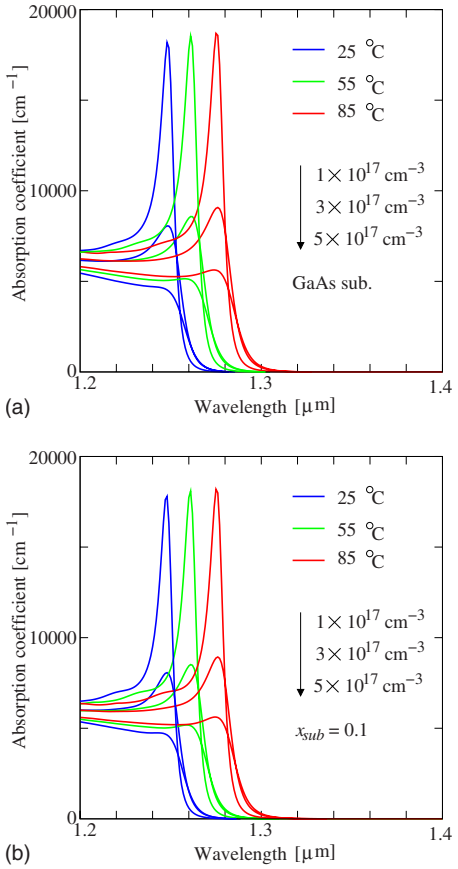

FIG. 2. (Color online) Absorption spectra of GaInAs/GaInAs QWs for the substrates with (a) x_{sub}=0 and (b) 0.1.

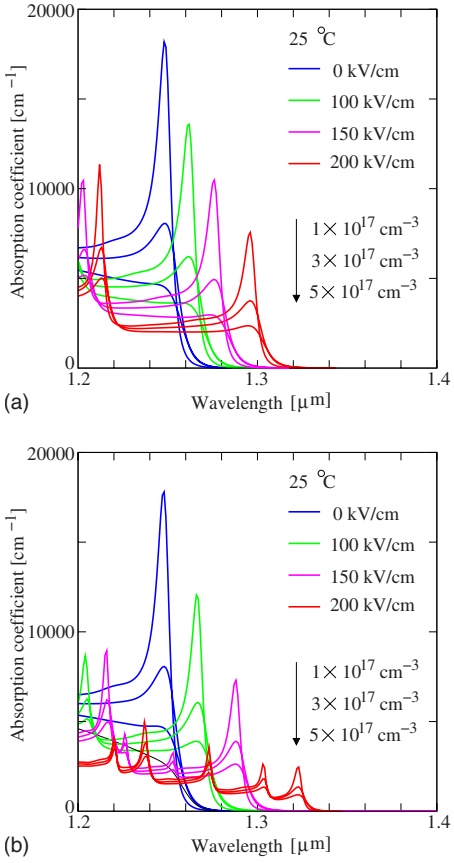

FIG. 4. (Color online) Absorption spectra for different bias electric fields for the substrates with (a) x_{sub}=0 and (b) 0.1.

coefficient does not change very much and the temperature dependence is similar to that of GaAs substrate. Figure 3 shows the absorption spectra of QWs at 25 °C for the substrates with x_{sub}=0, 0.1, and 0.2. For x_{sub}=0.2, the absorption coefficient is smaller than that of the other two. This is because as ΔE_c becomes smaller for larger values of x_{sub}, the overlap of wave function between conduction and valence bands becomes small.

Figures 4(a) and 4(b) show the absorption spectra of GaInAs/GaInAs QWs under different bias electric fields for the substrates with x_{sub}=0 and 0.1. Although at lower bias fields, the spectra are similar, a difference can be seen at high bias electric fields. The absorption coefficient of QWs with x_{sub}=0.1 at 200 kV/cm is significantly smaller than that of the GaAs substrate. This is explained by the wave function of the conduction band. Figures 5(a) and 5(b) show the wave function of the first conduction sub-band for the substrates with x_{sub}=0 and 0.1 under different electric fields. For the GaAs substrate, the wave function is well confined even under 200 kV/cm electric fields, while for x_{sub}=0.1, significant leakage can be seen. The leakage makes the overlap of wave functions between conduction and valence sub-bands very small, leading to smaller absorption coefficient.

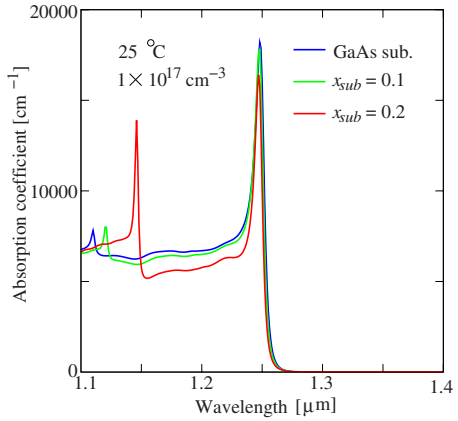

FIG. 3. (Color online) Absorption spectra of GaInAs/GaInAs QWs for different substrates.

B. GaInAs/AlGaInAs QWs

As shown in Figs. 5(a) and 5(b), the leakage of wave functions under the large bias electric fields can be suppressed for deep QWs (GaAs substrate). However, the strain for QWs on GaAs substrate [Fig. 5(a)] is larger than that of GaInAs substrate. To increase the depth of QWs without changing the strain, larger band gap material has to be used for barriers. Here, the effect of barrier material on the absorption spectra is investigated. The x_{sub} is fixed to 0.1. Figure 6(a) shows the potential distributions of GaInAs/AlGaInAs QWs for different barrier band gap wavelength, λ_B. For λ_B=0.85 μm, ΔE_c almost doubles, compared with that of GaInAs barrier. Figure 6(b) shows the wave functions of the first conduction sub-band under the bias electric field of 150 kV/cm. We can see that as λ_B increases, the confine-

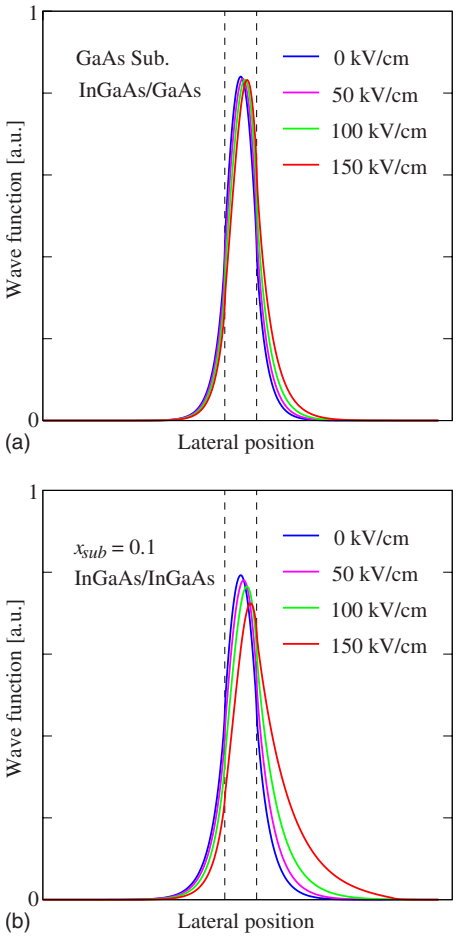

FIG. 5. (Color online) Wave function of the first conduction sub-band for different bias electric fields for the substrates with (a) x_{sub}=0 and (b) 0.1.

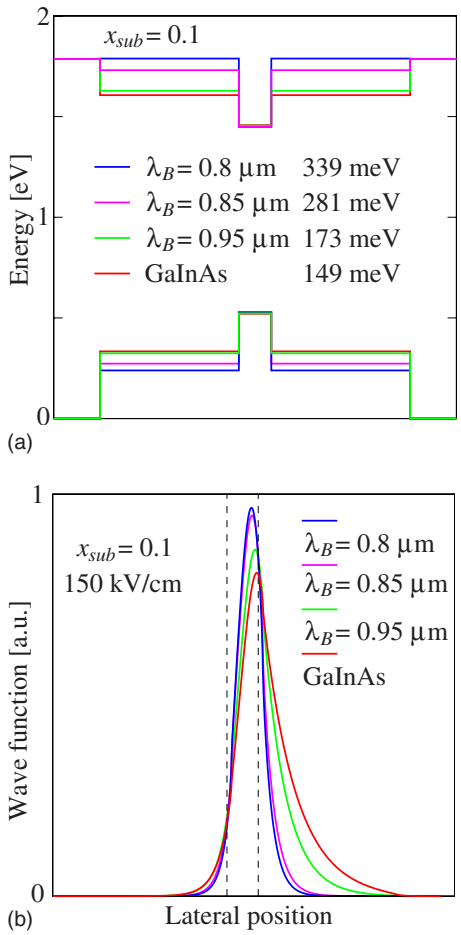

FIG. 6. (Color online) (a) Potential distributions of GaInAs/AlGaInAs QWs for the substrate with x_{sub}=0.1. (b) Wave function of the first conduction sub-band for the substrates with x_{sub}=0.1 at the bias electric field of 150 kV/cm.

ment becomes stronger. The strong confinement makes the overlap between the conduction and valence bands larger, leading to a larger absorption coefficient even under large bias electric fields. This is illustrated in Fig. 7, in which the absorption spectra of GaInAs/AlGaInAs QW with λ_B =0.85 μm are shown. For the bias electric field of 200 kV/cm, the difference from Fig. 4(b) is especially clear. A large absorption coefficient can be obtained for deep QWs under large bias fields. On the other hand, the redshift of the spectra is smaller for deep QWs due to their strong confinement.

C. GaInNAs/GaInAs QWs

As shown in the Sec. III B, by using ternary substrates, the strain in the well layer can be significantly reduced. However, strain of more than 2% is still required for x_{sub} =0.1. Here, the electroabsorption of GaInNAs/GaInAs QWs is investigated to determine whether the strain can be reduced further. Figure 8 shows the strain of 7 nm GaInNAs/GaInAs QWs as a function of the N mole fraction for achieving C1V1 wavelength of 1.24 μm. For x_{sub}=0.1, the strain is smaller than 1.5% when the N mole fraction is 1% to 2%, which are experimentally achieved values. Also, strain smaller than 1.5% is a typical value used in conventional QWs grown on InP substrates. Too much strain in QWs makes the crystal growth difficult and degrades the crystal quality and long-term reliability. Figure 9(a) shows the potential distributions of GaInNAs/GaInAs QWs with x_{sub} =0.1 for different values of ε_w. Nitrogen mole fractions are 0.88% and 1.49% for ε_w=1.5% and 1%. The ΔE_c does not change very much while ΔE_v is reduced for larger N mole fraction. Due to the interaction between the conduction and N-resonant bands, the energy of the first conduction sub-band is lower than the bottom of the conduction band potential as shown by dashed lines in Fig. 9(a). Therefore, effec-

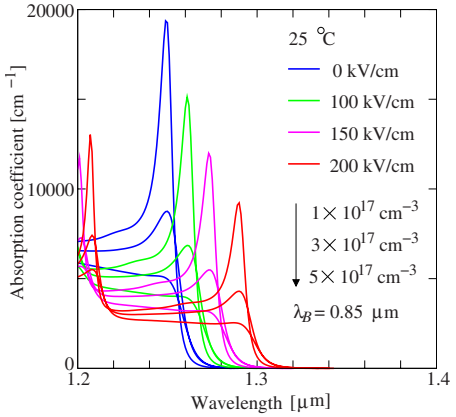

FIG. 7. (Color online) The absorption spectra of GaInAs/AlGaInAs QWs with λ_B=0.85 μm.

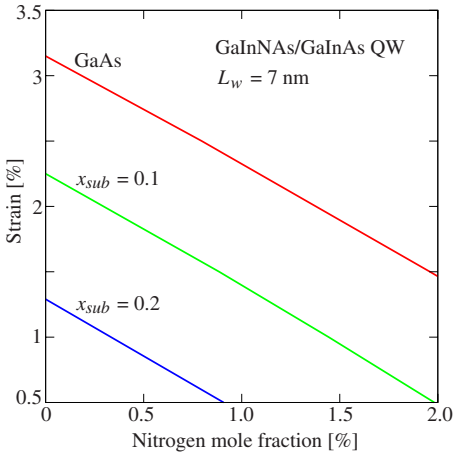

FIG. 8. (Color online) Strain of GaInNAs/GaInAs QWs as a function of N mole fraction for C1V1 wavelength of 1.24 μm.

tive QW depth is increased for smaller values of strain (larger N mole fraction). It should also be noted that smaller ΔE_v reduces the hole-pile-up effect under modulation and is therefore useful for high-speed modulators. The value of ΔE_v is around 100 meV, which is comparable to AlGaInAs based QWs grown on InP substrates. Therefore, the potential modulation speed is similar to that of conventional materials.

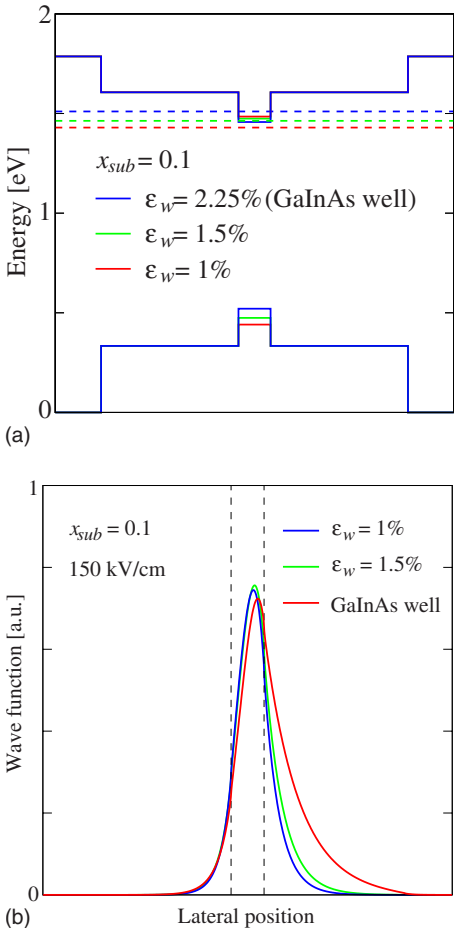

FIG. 9. (Color online) (a) Potential distributions of GaInNAs/GaInAs QWs. Dashed lines show the energy levels of first conduction sub-bands. (b) Wave function of the first conduction sub-band at the bias electric field of 150 kV/cm.

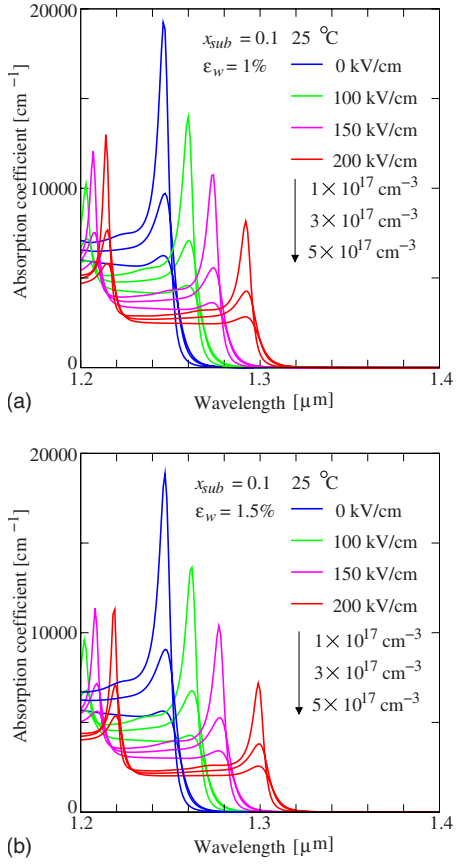

FIG. 10. (Color online) The absorption spectra of GaInNAs/GaInAs QWs with (a) ε_w=1% and (b) 1.5%.

Figure 9(b) shows the wave functions of first conduction sub-bands under the electric field of 150 kV/cm. It is clear that the confinement is stronger for QWs with a larger N mole fraction, which means the effective barrier height can be increased without using wide-band gap materials for barriers. Figures 10(a) and 10(b) show the absorption spectra of GaInNAs QWs with ε_w=1% and 1.5%. Since the confinement is similar between ε_w=1% and 1.5% as shown in Fig. 9(b), the absorption spectra are also similar and the difference with GaInAs QWs [Fig. 4(b)] is clear at large electric fields. Recently, the electroabsorption of GaInNAs QWs grown on GaAs substrate was reported.[28,29] Although GaAs substrates are easily available and the results showed that the usefulness of these materials for EAMs, the required strain is around 2% for typical values of N mole fraction of 1% to 1.5% (Fig. 8). If we consider the integration with laser diodes, which is the current trend for EAM based lightsources,[3–5] the situation becomes worse. Since the lasing wavelength has to be longer than the band edge wavelength of EAMs, larger strain is necessary in the laser section. Large strain makes it difficult to grow a large number of wells and degrades the long-term reliability. While GaInAs or quasi-GaInAs substrate is difficult to fabricate compared with GaAs, they have superiority in terms of strain.

IV. EXTINCTION RATIO (ER) OF EAMS

The ER is one of the most important parameters for characterizing EAMs. Here, the ERs of GaInAs and GaIn-

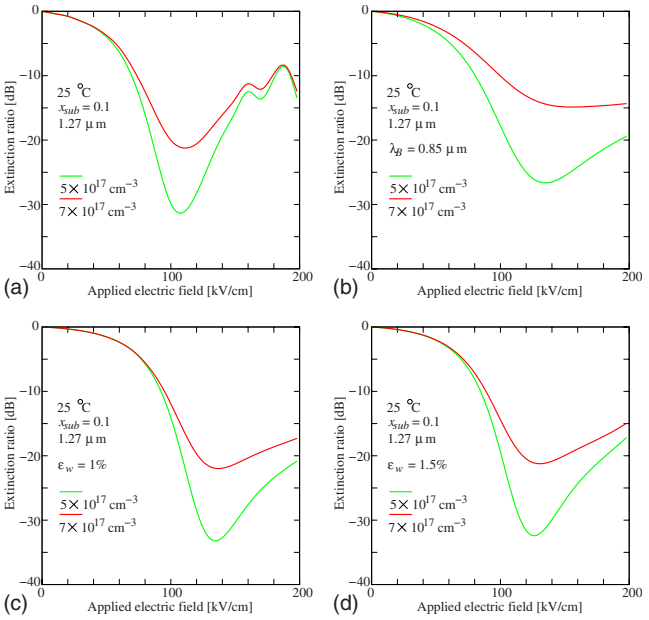

FIG. 11. (Color online) ER of (a) GaInAs/GaInAs, (b) GaInAs/AlGaInAs, (c) GaInNAs/GaInAs (ε_w=1%), and (d) GaInNAs/GaInAs (ε_w=1.5%) QWs.

NAs QWs are discussed. The layer structure considered here is as follows: six QWs with 7 nm well, a 10 nm barrier, and a 240 nm GaInAs separate confinement heterostructure layer, sandwiched between p- and n-GaInP claddings. This is the experimentally acheived structure in Ref. 17 with ε_w exceeding 2%. Finite-element calculation gives the confinement factor, Γ, of 0.103, and we assume the modulator length, L_{EA}, of 200 μm. The ER in dB units is given by

$$\mathrm{ER} = 10 \log_{10}[-\Gamma \alpha(\lambda, F) L_{\mathrm{EA}}], \tag{3}$$

where α is the absorption coefficient, λ is the incident wavelength which is taken as 1.27 μm here, and F is the bias electric field. The x_{sub} is fixed to 0.1 and the temperature is 25 °C. Figure 11(a) shows the ER of a GaInAs/GaInAs QW. A strong absorption peak due to excitons can be seen and the ER becomes smaller for larger values of applied fields, reflecting the small α at the large bias fields as shown in Fig. 4(b). It should be noted that it is normally difficult to observe the exciton peak in the ER of EAMs in experiment for various reasons, such as increased carrier density in the well at high bias voltage (photon absorption generates electron-hole pairs) and experimentally induced broadening. Therefore, the ER shown in Fig. 11(a) may become smaller in a fabricated device since the exciton absorption is dominant in this QW. Figure 11(b) shows the ER of a GaInAs/AlGaInAs QW with λ_B=0.85 μm. In contrast to Fig. 11(a), a large ER is obtained for larger values of electric fields. Since the dominant mechanism in this range is band-to-band absorption, the effect of experimental broadening is small compared with that of exciton absorption. Figures 11(c) and 11(d) show the ER of GaInNAs/GaInAs QWs with ε_w=1% and 1.5%. The characteristics are similar to those seen in Fig. 11(b), because an effectively deep QW is formed due to the interaction with the N-resonant band. In this case, the QWs are Al-free, which leads to easier crystal growth and processing and higher reliability. Further, more than a 1% reduction in the strain is possible and more wells can be grown. This means that larger ER can be obtained for the same modulator length or the same ER can be obtained for shorter modulator length, leading to large electro/optical bandwidth due to a reduced capacitance, which is suitable for high-speed modulators. If a ridge waveguide structure buried with a benzocyclobutene[3–5] is employed, the parasitic capacitance can be significantly reduced compared with that of a buried waveguide structure. Since the modulator length can be comparable to that of conventional EAMs, the parasitic capacitance is similar, indicating a possibility of 25 and even 40 Gbit/s operation.[3–5] It should be noted that EAMs considered in this paper are highly polarization dependent. Since only compressive strain is allowed for this material system to obtain 1.3 μm light, it seems to be difficult to achieve polarization insensitivity by simple QW design.[11] However, if we consider the integration with laser diodes,[3–5] the polarization sensitivity does not matter.

V. CONCLUSION

We investigated electroabsorption in highly strained GaInNAs QWs grown on GaInAs ternary substrates. Microscopic many-body theory was used to exclude theoretical uncertainty and take into account physical phenomena associated with the correlation effects in semiconductors. Calculated results show that under high electric fields, the absorption coefficient of QWs with large x_{sub} becomes small due to small overlap integral of wave functions between the conduction and valence bands. With GaInNAs QWs, the effective barrier height becomes large due to the interaction with the N-resonant band and a larger absorption coefficient is obtained under large bias electric fields. These QWs also enable us to make an Al-free EAM with reduced strain, which is preferable for easier crystal growth and processing and for improving reliability.

[1] http://www.ieee802.org/3/ba/
[2] H. Hayashi, S. Makino, T. Kitatani, T. Shiota, K. Shinoda, S. Tanaka, M. Aoki, N. Sasada, and K. Naoe, Proceedings of 2008 European Conference and Exhibition on Optical Communication, 2008, We.3.C.3.
[3] W. Kobayashi, M. Arai, T. Yamanaka, N. Fujiwara, T. Fujisawa, M. Ishikawa, K. Tsuzuki, Y. Shibata, Y. Kondo, and F. Kano, IEEE Photon. Technol. Lett. **21**, 1054 (2009).
[4] T. Fujisawa, M. Arai, N. Fujiwara, W. Kobayashi, T. Tadokoro, K. Tsuzuki, Y. Akage, R. Iga, T. Yamanaka, and F. Kano, IEEE Electron Device Lett. **45**, 900 (2009).
[5] W. Kobayashi, T. Yamanaka, M. Arai, N. Fujiwara, T. Fujisawa, K. Tsuzuki, T. Ito, T. Tadokoro, and F. Kano, IEEE Photon. Technol. Lett. **21**, 1317 (2009).
[6] H. Ishikawa, Appl. Phys. Lett. **63**, 712 (1993).
[7] H. Ishikawa and I. Suemune, IEEE Photon. Technol. Lett. **6**, 344 (1994).
[8] H. Ishikawa and I. Suemune, IEEE Photon. Technol. Lett. **6**, 1315 (1994).
[9] K. Otsubo, H. Shoji, T. Kusunoki, T. Suzuki, T. Uchida, Y. Nishijima, K. Nakajima, and H. Ishikawa, IEEE Photon. Technol. Lett. **10**, 1073 (1998).
[10] K. Otsubo, H. Shoji, T. Kusunoki, T. Suzuki, T. Uchida, Y. Nishijima, K. Nakajima, and H. Ishikawa, Electron. Lett. **33**, 1795 (1997).
[11] D. Alexandropoulos, M. J. Adams, Z. Hatzopoulos, and D. Syvridis, IEEE J. Quantum Electron. **41**, 817 (2005).
[12] M. Arai, T. Watanabe, M. Yuda, K. Kinoshita, S. Yoda, and Y. Kondo, IEEE J. Sel. Top. Quantum Electron. **13**, 1295 (2007).
[13] T. Fujisawa, M. Arai, T. Kakitsuka, T. Yamanaka, Y. Kondo, and H. Yasaka, Appl. Phys. Express **1**, 041203 (2008).
[14] M. Arai, T. Fujisawa, W. Kobayashi, K. Nakashima, M. Yuda, and Y.

Kondo, Electron. Lett. **44**, 1359 (2008).
[15]M. Arai, W. Kobayashi, T. Fujisawa, M. Yuda, T. Tadokoro, K. Kinoshita, S. Yoda, and Y. Kondo, Appl. Phys. Express **2**, 022101 (2009).
[16]M. Arai, T. Tadokoro, T. Fujisawa, W. Kobayashi, K. Nakashima, M. Yuda, and Y. Kondo, Electron. Lett. **45**, 359 (2009).
[17]M. Arai, T. Tadokoro, T. Fujisawa, W. Kobayashi, K. Nakashima, M. Yuda, and Y. Kondo, IEEE Photon. Technol. Lett. **21**, 1344 (2009).
[18]M. Kondow, T. Kitatani, S. Nakatsuka, M. C. Larson, K. Nakahara, Y. Yazawa, M. Okai, and K. Uomi, IEEE J. Sel. Top. Quantum Electron. **3**, 719 (1997).
[19]M. Hofmann, A. Wagner, C. Ellmers, C. Schlichenmeier, S. Schafer, F. Hohnsdorf, J. Koch, W. Stolz, S. W. Koch, W. W. Ruhle, J. Hader, J. V. Moloney, E. P. O'Reilly, B. Borchert, A. Y. Egorov, and H. Riechert, Appl. Phys. Lett. **78**, 3009 (2001).
[20]S. Tomic, E. P. O'Reilly, R. Fehse, S. J. Sweeney, A. R. Adams, A. D. Andreev, S. A. Choulis, T. J. C. Hoesa, and H. Riechert, IEEE J. Sel. Top. Quantum Electron. **9**, 1228 (2003).
[21]J. Hader, S. W. Koch, and J. V. Moloney, Solid-State Electron. **47**, 513 (2003).
[22]W. W. Chow, A. Knorr, S. Hughes, A. Girndt, and S. W. Koch, IEEE J. Sel. Top. Quantum Electron. **3**, 136 (1997).
[23]W. W. Chow and S. W. Koch, *Semiconductor-laser fundamentals* (Springer, New York, 1999).
[24]J. Hader, J. V. Moloney, S. W. Koch, and W. W. Chow, IEEE J. Sel. Top. Quantum Electron. **9**, 688 (2003).
[25]T. Fujisawa, M. Arai, T. Yamanaka, Y. Kondo, and F. Kano, J. Appl. Phys. **105**, 113114 (2009).
[26]T. Fujisawa, T. Sato, M. Mitsuhara, T. Kakitsuka, T. Yamanaka, Y. Kondo, and F. Kano, IEEE J. Quantum Electron. **45**, 1183 (2009).
[27]I. Vurgaftman, J. R. Meyer, and L. R. Ram-Mohan, J. Appl. Phys. **89**, 5815 (2001).
[28]J. B. Héroux, X. Yang, and W. I. Wang, IET Optoelectron. **150**, 92 (2003).
[29]V. Lordi, H. B. Yuen, S. R. Bank, and J. S. Harris, Appl. Phys. Lett. **85**, 902 (2004).